2

INJURY BIOMECHANICS RESEARCH
Proceedings of the Thirty-fifth International Workshop

Determining Non-Censored Rib Fracture Data During Side Impact Loading

A. R. Kemper, C. McNally, S. J. Manoogian, and S. M. Duma

Virginia Tech – Wake Forest, Center for Injury Biomechanics

ABSTRACT

The purpose of this paper is to present a method to determine the timing of individual rib fractures during dynamic side impact tests on human cadavers. The technique utilizes a total of 18 single axis strain gages placed throughout the thorax. Specifically, single axis strain gages were placed on ribs three through eight on the left and right lateral portions of the thorax, as well as the posterior portion of the impacted side. By utilizing this technique, the exact timing of an injury level can be characterized relative to the mechanical parameters. In order to simulate thoracic side impact loading from a severe car crash, a custom pneumatic impactor was designed and fabricated. The thoracic testing was conducted at an impact speed of 12 m/s and an impactor mass of 23.4 kg. The impacting surface was a flat rigid plate, with a length of 41.5 cm and a width of 25.5 cm, instrumented with a load cell and accelerometer. Thoracic rods attached to ribs five, seven, and nine were used along with potentiometers to measure lateral chest compression. All data was sampled at 15 kHz. The time histories of each strain gage were analyzed to determine the time of fracture which could then be compared directly to the chest compression at that exact time of each rib fracture, thereby creating a non-censored data set. Lateral fractures on the impacted side occurred between 2% and 9% of compression measured at rib 5. Posterior fractures on the impacted side occurred between 8% and 16% compression measured at rib 5. Lateral fractures on the non-impacted side occurred between 28 % and 32% compression measured at rib 5. Finally, the primary loading mode of the ribs varied with respect to thoracic region. The exterior portion of the ribs on the lateral region of both the impacted and non-impacted side was placed in compression, while the posterior region of the impacted side was placed in tension. The peak strain at failure ranged from -4192 mstr to -20194 mstr for lateral portions of the thorax and from 7491 mstr to 14142 mstr for posterior portions of the thorax. Using rib fractures as the parameter for AIS scores, it was found that AIS=1 injuries occurred at a chest compressions of 2% to 3%, AIS=2 at 4% to 7%, AIS=3 at 7% to 9% measured at rib five. It is expected that this data will augment and clarify the foundation of thoracic injury risk functions for side impact.

INTRODUCTION

Approximately 10,000 fatalities occur annually due to automobile side impact collisions (Kuppa et al., 2003). It has been reported that thoracic injuries are the most common serious injury (AIS≥3) to vehicle occupants in non-rollover near side crashes (Samaha et al., 2003). In side impact laboratory studies, rib fractures are the most frequent MAIS injury and therefore are the primary basis of current side impact thoracic injury criteria (Kuppa et al., 2003; Pintar et al., 1997; Viano, 1989; Morgan et al., 1986). However, previous studies aimed at determining thoracic injury criteria in side impacts rely on impact tests that only provide censored injury data. In other words,

one only knows that an injury occurred at some point during the impact test. Therefore, it is not possible to determine the exact loads, accelerations, or displacements at the time of injury. In order to reduce this limitation, this study presents a method to generate non-censored rib fracture data resulting from side impact loading.

METHODS

Subject Information

A total of two fresh frozen human male cadavers, approximately 50th percentile male, were used in the current study. Subject information and anthropometric measurements from each cadaver were recorded (Table 1). It should be noted that chest depth and circumference measurements include the skin and soft tissue, while the chest width measurements do not. The left hand of the cadavers was x-rayed, scanned and processed by CompuMed incorporated (Los Angeles, CA). This type of BMD measurement, however, only provides an indication of overall bone strength and does not account for local changes in bone density or composition. Therefore, the BMD obtained through this method is referred to as the "global BMD". The T-score is used to compare the cadaver's global BMD with that of the "young" normal population, using 30 years of age as the comparison. The Z-score is used to compare the global BMD of the subjects with the average for their age. Normal bone has a T-score of better than -1.0, Osteopenia or low bone mass is classified with T-scores between -1.0 and -2.5, and osteoporosis is indicated by T-scores of lower than - 2.5.

Table 1. Subject information and anthropometric data.

Test Measurement			**Subject ID**	
			1	**2**
General	Age	(yr)	56	49
	Weight	(kg)	63.2	71.8
	Height	(cm)	165.0	170.0
	Global BMD	-	90.1	109.4
	T- Score	-	-1.9	-0.1
	Z- Score	-	-1.0	0.3
Thorax	Thorax depth (mid-sternum)	(cm)	22.4	24.4
	Thorax circumference (mid-sternum)	(cm)	86.4	88.9
	Chest width at rib 5	(cm)	26.2	26.2
	Chest width at rib 7	(cm)	26.9	27.7
	Chest width at rib 9	(cm)	27.9	28.7

Instrumentation

The cadavers were instrumented with 15 single axis accelerometers, 18 thoracic strain gages, 3 thoracic rods, and 22 photo targets prior to testing (Figures 1, 2, and 3). All accelerometers and photo targets were rigidly attached to boney structures using bone screws. Cadaver accelerations were recorded with single axis accelerometers (Endevco 7264B, 2000 G, San Juan Capistrano, CA) mounted to three axis cubes on the head, sternum, T1, T12, and sacrum (Figure 1). Photo targets were placed on the head, sternum, T1, T4, T7, T10, T12, L1, L5, sacrum, and ilium. The lateral thoracic displacement was measured by placing rods through the thorax (Figure 2). The rods were attached to the interior portion of the rib on the impacted side. On the opposite side the rods were attached to string potentiometers (Space Age Control Inc. 160-1705, 539.75mm, Palmdale, CA), which were rigidly attached to the thorax with a custom mounting plate. As the thorax is compressed laterally, the rods are pushed out of the thorax which causes the potentiometer cable to spoil out and measure compression. It should be noted that because the thoracic rods used to measure compression were attached to the interior portion of the struck ribs, the compression measurement does not include the compression of the skin, soft tissue, or clothing surrounding the exterior portion of the thorax.

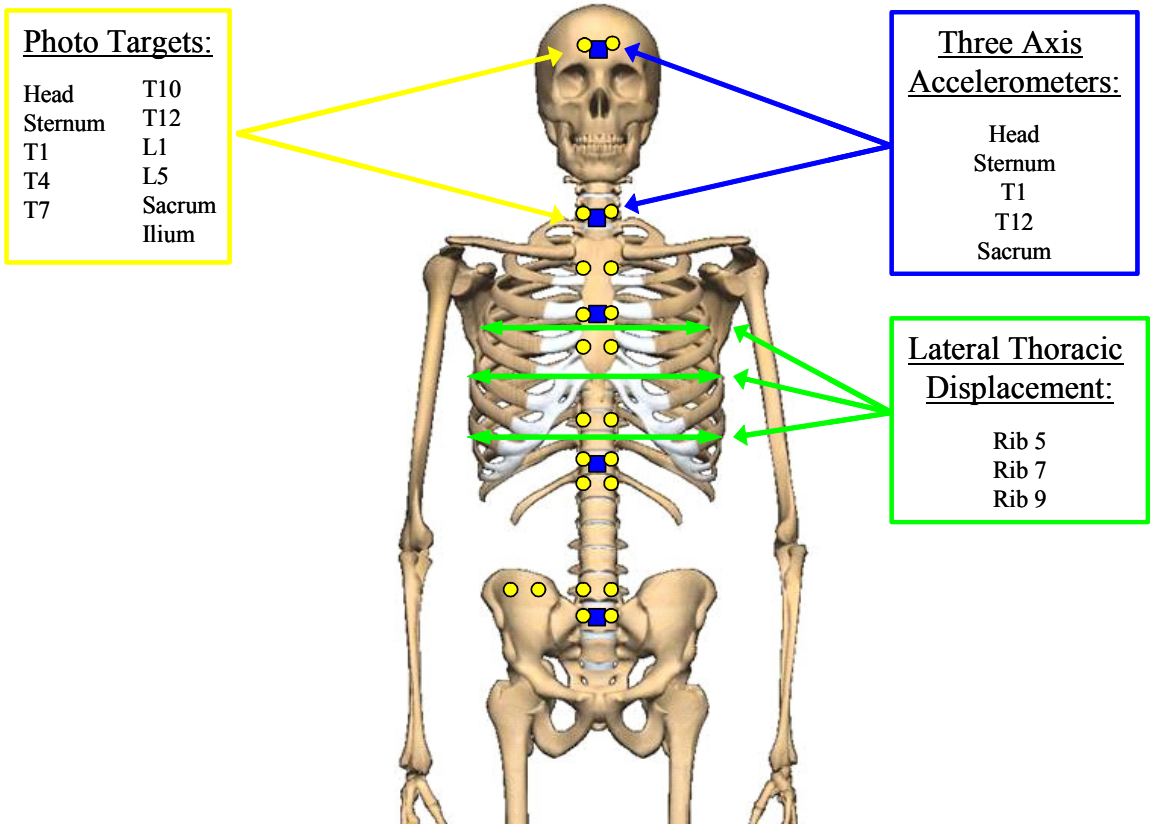

Figure 1: Location of photo targets, accelerometers, and chest compression.

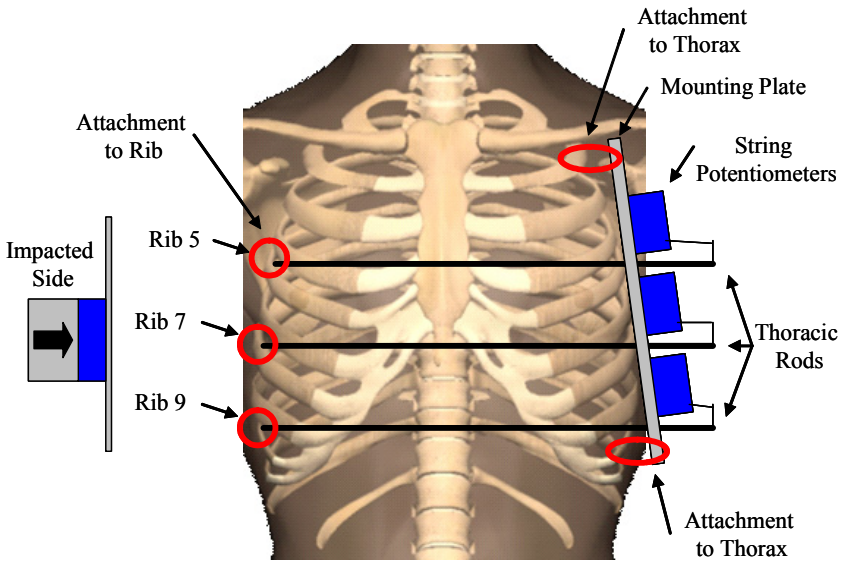

Figure 2: Thoracic displacement measurement methodology.

A total of 18 single axis strain gages (Vishay Micro-Measurement, CEA-06-062UW-350, Shelton, CT) were applied to the exterior of: the right and left lateral region of ribs 3 through 8, and the right posterior region of ribs 3 through 8 (Figure 3). Once the location of each strain gage was determined the soft tissue and periosteum was removed, and the bone was swabbed with ether to locally dry the bone. Upon drying, an acidic solution (Vishay Micro-Measurement, Conditioner A, Shelton, CT) was applied to the surface with a clean piece of gauze in order to etch the surface of the bone. Then basic solution (Vishay Micro-Measurement, Neutralizer 5A, Shelton, CT), was applied to the surface in order to neutralize the acidic solution. The gage was removed from its case and prepared by applying catalyst (Vishay Micro-Measurement, M-Bond Catalyst, Shelton, CT) to the underside of the gage. Next, an adhesive (Vishay Micro-Measurement, M-Bond 200 Adhesive, Shelton, CT) was applied to the bone and the gage was quickly pushed over the adhesive in a rolling manner. The strain gage was covered with a small piece of latex and held with firm pressure for 3 minutes (Figure 4). Special care was taken to align each gage so that it was in line with the axis of the rib. Finally, the strain gage wire was strain relieved with a zip tie placed around the rib.

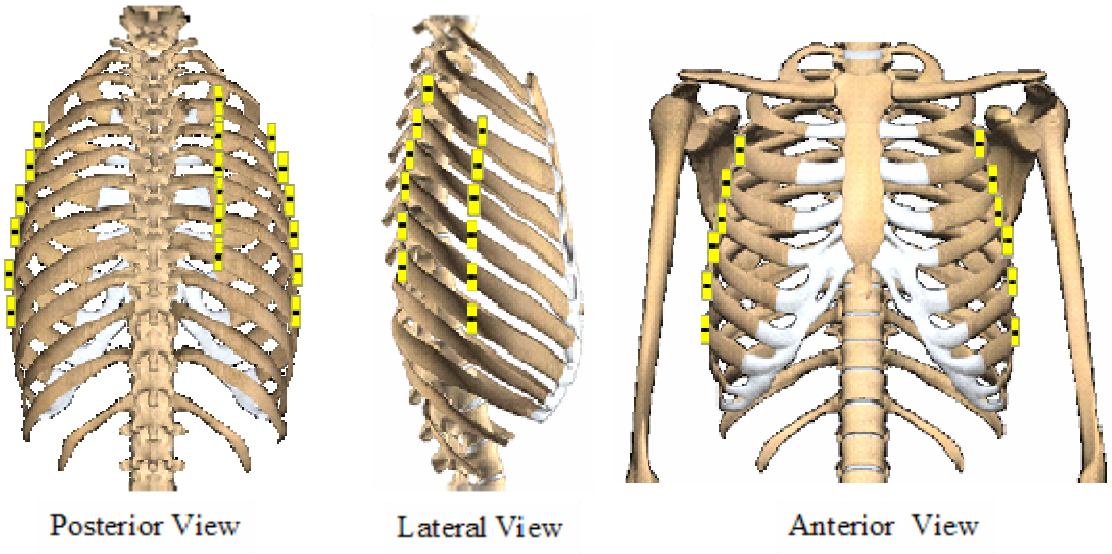

Figure 3: Thoracic strain gage locations.

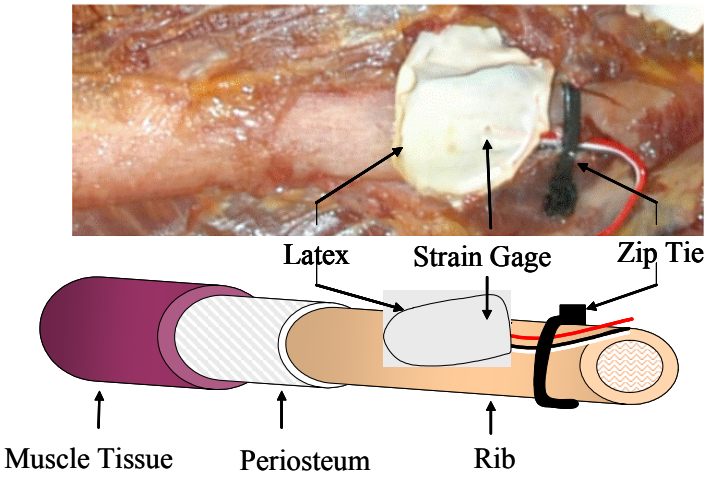

Figure 4: Thoracic strain gage attachment.

Experimental Setup

The primary component of the side impact experimental setup was a custom pneumatic impactor. A custom testing seat was designed and fabricated to allow a cadaver to be placed in a seated position (Figure 5). The use of an adjustable back support bar allowed for a clear line of sight to the posterior photo targets, while maintaining the normal posture and upper body load on the pelvis and spine (Cavanaugh et al., 1993). A Teflon ® sheet was placed between the cadaver and the seat pan to minimize friction (Cavanaugh et al., 1993).

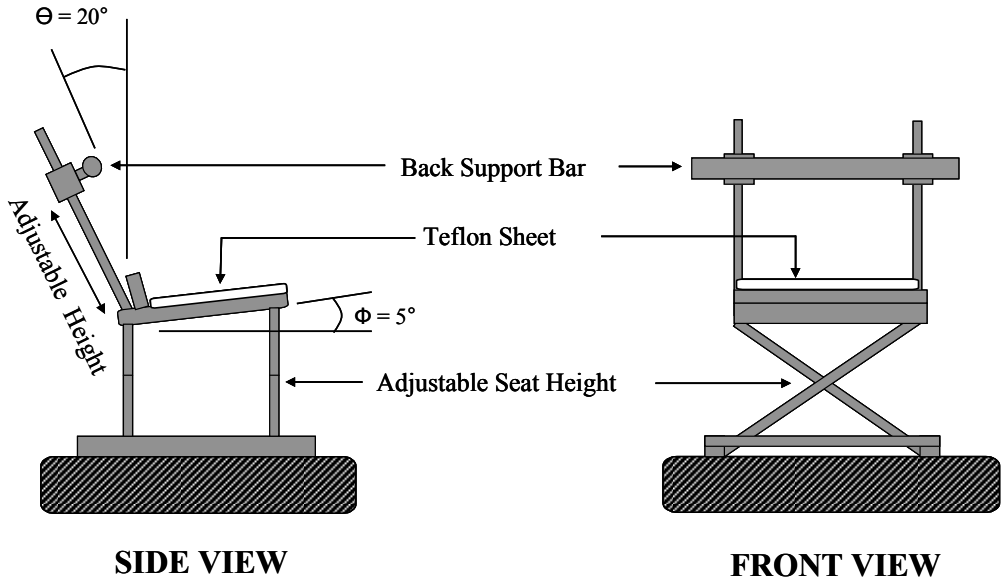

Figure 5: Custom side impact testing seat.

Once the cadaver was placed in the appropriate seated position, the arm was placed in the desired position with an overhead rope. It should be noted that, the head was held back with a piece of masking tape, which had been slightly cut to ensure it would tear free during the test event. The impacting surface was a flat rigid plate with a height of 41.5 cm and a width of 25.5 cm (Figure 6). Special care was taken to insure the impacting plate did not strike the pelvis. The impactor was instrumented with a five axis load cell (Robert A. Denton, Inc. 1968, 22,240 N, Rochester Hills, MI) and a single axis accelerometer (Endevco 7264B, 2000 G, San Juan Capistrano, CA). The impactor stroke was set to be 250 mm for both destructive tests. The destructive thoracic testing was conducted at an impact speed of 12 m/s and an impactor mass of 23.4 kg. The data was sampled at 15 kHz for all tests. Force, displacement, and accelerometer data were filtered to Channel Filter Class (CFC) 180, while strain gage data was not filtered. Two high speed video cameras recorded the event from different angles (front and back view) at 1000 fps.

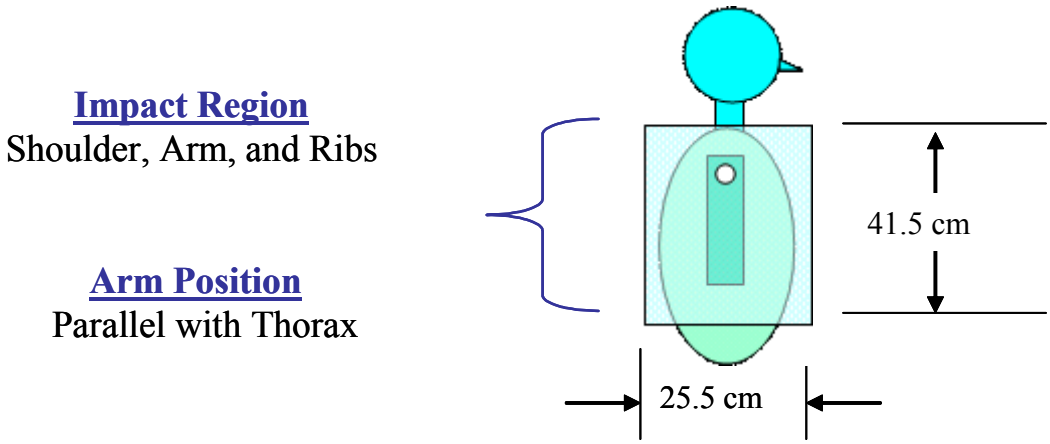

Figure 6: Thoracic impact areas and arm position.

RESULTS

Rib Fracture Identification

The rib fractures locations were determined by performing a post-test injury analysis on each cadaver using a detailed necropsy of the thorax. The fracture locations were photographed and documented for each cadaver (Figures 7 and 8, Tables 2 and 3). Cadaver_1 sustained a total of ten (n=10) rib fractures, one (n=1) clavicle fracture, and one (n=1) clavicle dislocation (Figure 7 and Table 2). An Abbreviated Injury Score (AIS) score of 3 was assigned to the rib cage of cadaver_1 based on the number and locations of rib fractures. Cadaver_2 sustained a total of ten (n=10) rib fractures and one (n=1) clavicle dislocation (Figure 8 and Table 3). An Abbreviated Injury Score (AIS) score of 3 was assigned to the rib cage of cadaver_2 based on the number and locations of rib fractures. There were no observed injuries to the shoulder joint, humerus, spine, or internal organs for either cadaver.

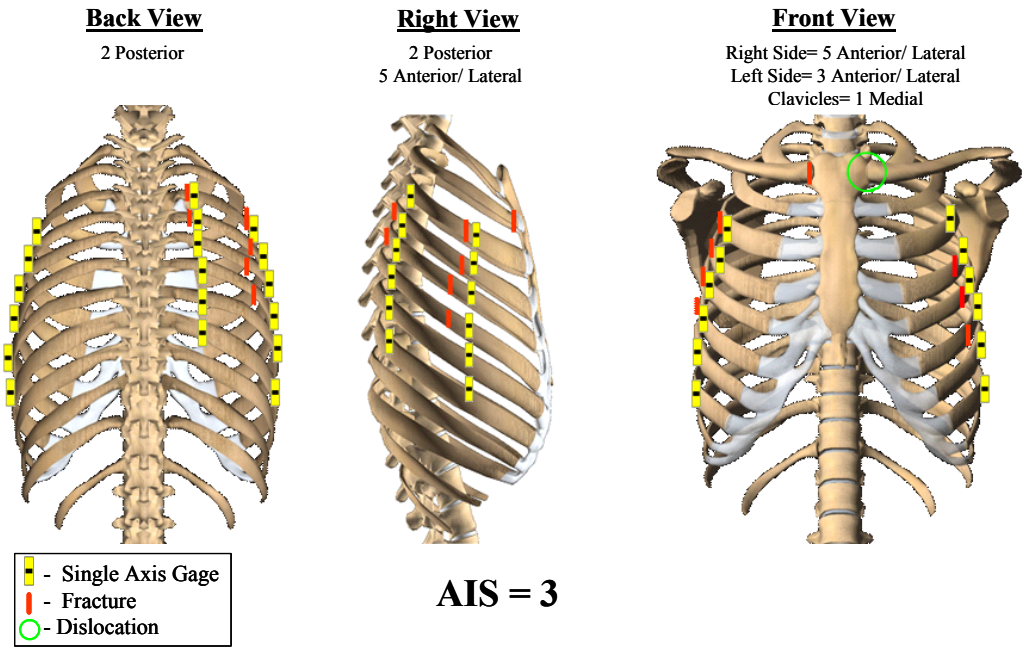

Figure 7: Rib fracture and strain gage locations for cadaver_1.

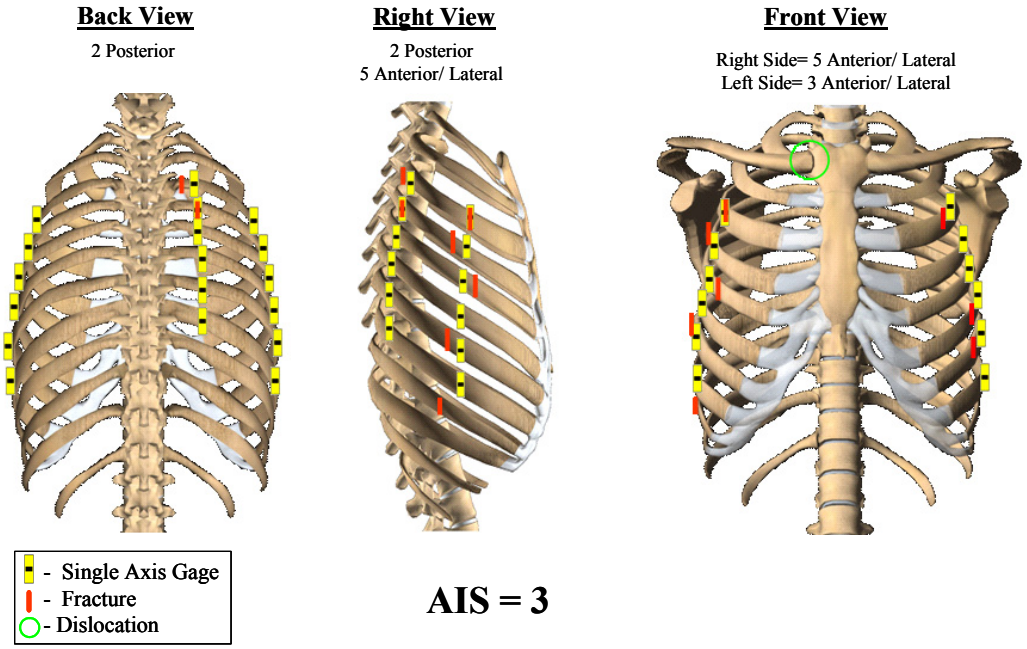

Figure 8: Rib fracture and strain gage locations for cadaver_2.

Rib Fracture Timing

The time at which each rib facture occurred was determined from the plots of strain gage output vs. time (Figure 9). The time histories of each strain gage were analyzed to determine the time of fracture which could then be compared directly to the impactor load or chest compression at that exact time, thereby creating a non-censored data set (Tables 2 and 3). Cadaver_2 sustained two fractures directly under strain gages. The fractures that occurred directly under gages are of particular interest because the failure strain at the time of fracture could be obtained from these gages.

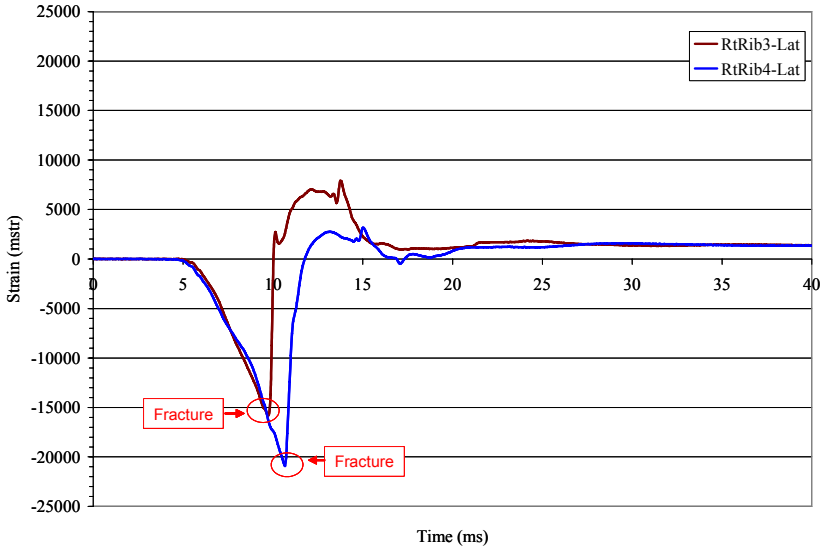

Figure 9: Determination of rib fracture timing.

Table 2. Rib fracture locations, fracture time, strain, and chest compression for cadaver_1.

Strain at Fracture		Fracture Location	Time	Strain at Time of Fracture	Upper Compression (Rib 5)	Middle Compression (Rib 7)	Lower Compression (Rib 9)
			ms	mstr	mm	mm	mm
Lateral Impacted Side	1	No Fracture	----	----	----	----	----
	2	51 mm to sternum center	N/G	N/G	N/G	N/G	N/G
	3	13 mm posterior of gage	7.87	-16220	19.4	12.5	1.2
	4	20 mm posterior of gage	8.20	-11184	22.3	15.0	1.9
	5	55 mm posterior of gage	6.40	-6501	7.6	3.5	0.1
	6	45 mm posterior of gage	B/G	B/G	B/G	B/G	B/G
	7	No Fracture	----	----	----	----	----
	8	No Fracture	----	----	----	----	----
	9	No Fracture	----	----	----	----	----
	10	No Fracture	----	----	----	----	----
Posterior Impacted Side	1	No Fracture	----	----	----	----	----
	2	No Fracture	----	----	----	----	----
	3	10 mm posterior of gage	8.07	7491	21.1	14.0	1.6
	4	10 mm posterior of gage	10.60	11350	42.0	33.5	12.6
	5	No Fracture	----	----	----	----	----
	6	No Fracture	----	----	----	----	----
	7	No Fracture	----	----	----	----	----
	8	No Fracture	----	----	----	----	----
	9	No Fracture	----	----	----	----	----
	10	No Fracture	----	----	----	----	----
Left Non-Impacted Side	1	No Fracture	----	----	----	----	----
	2	No Fracture	----	----	----	----	----
	3	No Fracture	----	----	----	----	----
	4	22 mm anterior of gage	18.27	-4787	80.3	73.4	42.0
	5	10 mm anterior of gage	16.80	-8540	76.4	68.1	37.6
	6	11 mm anterior of gage	19.60	-7668	82.6	77.2	45.8
	7	No Fracture	----	----	----	----	----
	8	No Fracture	----	----	----	----	----
	9	No Fracture	----	----	----	----	----
	10	No Fracture	----	----	----	----	----

Note: N/G= Not Gaged; B/G= Broken Gage; N/A= Not Applicable

Table 3. Rib fracture locations, fracture time, strain, and chest compression for cadaver_2.

Region and Rib Number		Fracture Location	Time	Strain at Time of Fracture	Upper Compression (Rib 5)	Middle Compression (Rib 7)	Lower Compression (Rib 9)
			ms	mstr	mm	mm	mm
Lateral Impacted Side	1	No Fracture	----	----	----	----	----
	2	No Fracture	----	----	----	----	----
	3	**immediately under gage**	9.67	-15680	11.1	12.1	0.0
	4	13 mm posterior of gage	10.67	-20914	17.1	19.5	0.9
	5	19 mm anterior of gage	8.47	-4192	4.8	4.1	0.0
	6	No Fracture	----	----	----	----	----
	7	19 mm anterior of gage	10.67	-8664	17.1	19.5	0.9
	8	No Fracture	----	----	----	----	----
	9	171 from sternum center	N/G	N/G	N/G	N/G	N/G
	10	No Fracture	----	----	----	----	----
Posterior Impacted Side	1	No Fracture	----	----	----	----	----
	2	No Fracture	----	----	----	----	----
	3	25 mm medial of gage	13.14	9801	34.3	35.0	14.0
	4	**immediately under gage**	14.40	14142	42.2	41.9	23.3
	5	No Fracture	----	----	----	----	----
	6	No Fracture	----	----	----	----	----
	7	No Fracture	----	----	----	----	----
	8	No Fracture	----	----	----	----	----
	9	No Fracture	----	----	----	----	----
	10	No Fracture	----	----	----	----	----
Left Non-Impacted Side	1	No Fracture	----	----	----	----	----
	2	No Fracture	----	----	----	----	----
	3	5 mm anterior of gage	21.07	-17424	72.0	67.7	64.8
	4	No Fracture	----	----	----	----	----
	5	No Fracture	----	----	----	----	----
	6	20 mm anterior of gage	22.14	-6261	74.4	69.6	69.4
	7	18 mm anterior of gage	22.07	-4828	74.2	69.5	69.2
	8	none	----	----	----	----	----
	9	none	----	----	----	----	----
	10	none	----	----	----	----	----

Note: N/G= Not Gaged; B/G= Broken Gage; N/A= Not Applicable

DISCUSSION

In order to illustrate the usefulness of the non-censored data, the percent chest deflection data was plotted vs. time with the fracture timing and corresponding Abbreviated Injury Scale (AIS) score (Figures 10 and 11). In both cadavers, all rib fractures occurred within 33% compression of the thorax. Lateral fractures on the impacted side occurred between 2% and 9% of compression measured at rib 5. Posterior fractures on the impacted side occurred between 8% and 16% compression measured at rib 5. Lateral fractures on the non-impacted side occurred between 28% and 32% compression measured at rib 5. Using rib fractures as the parameter for AIS scores, it was found that AIS=1 injuries occurred at a chest compressions of 2% to 3%, AIS=2 at 4% to 7%, and AIS=3 at 7% to 9% measured at rib five. It should be noted that because the thoracic rods used to measure compression were attached to the interior portion of the struck ribs, the compression measurement does not include the compression of the skin, soft tissue, or clothing surrounding the exterior portion of the thorax.

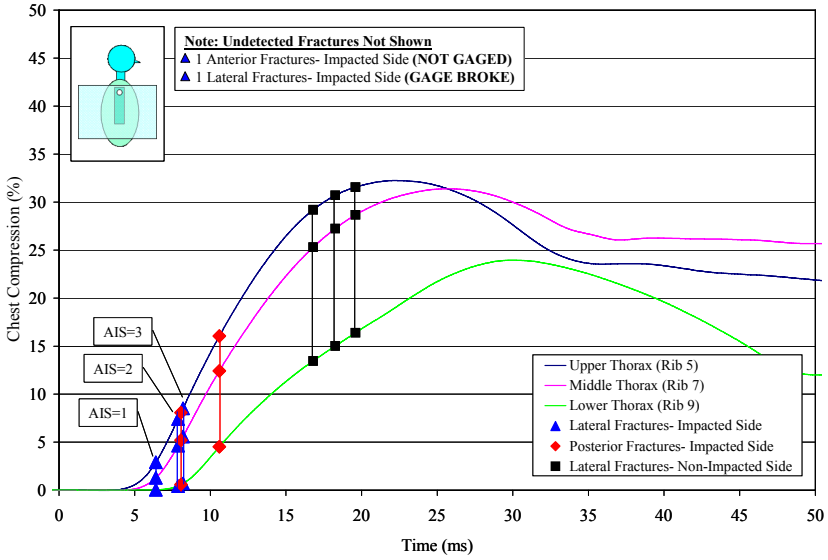

Figure 10**:** Cadaver_1 rib fracture timing.

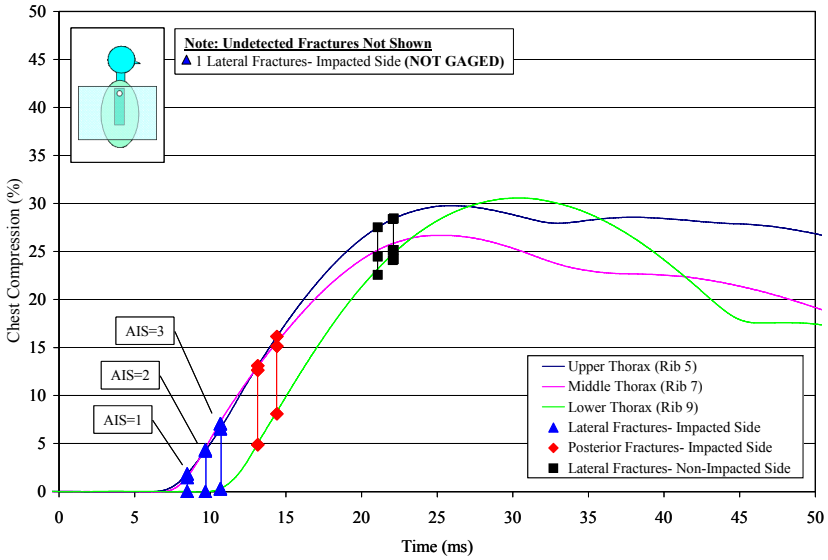

Figure 11: Cadaver_2 rib fracture timing.

The primary loading mode of the ribs was found to vary with respect to thoracic region (Figures 12 and 13). The exterior portion of the ribs on the lateral region of both the impacted and non-impacted side was placed in compression, while the exterior portion of the posterior region of the impacted side was placed in tension.

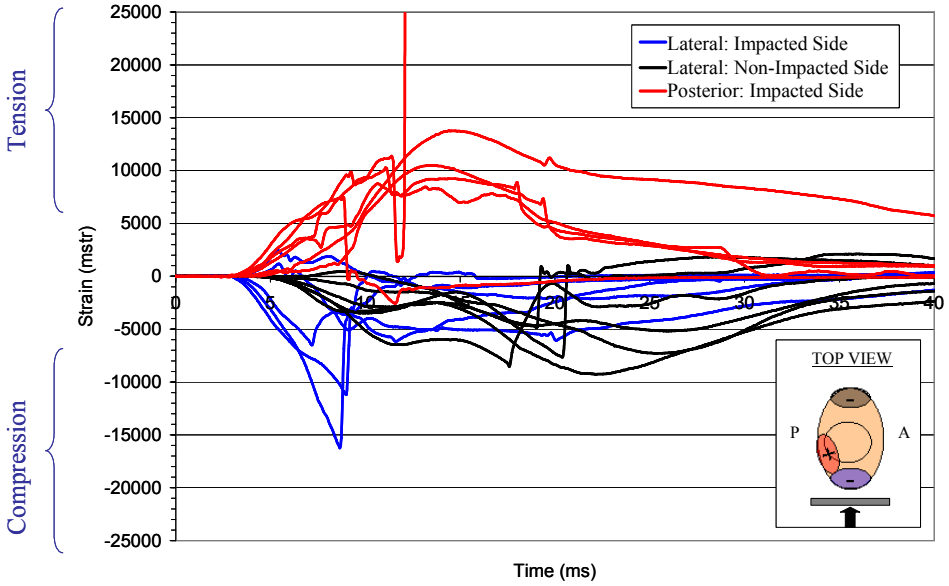

Figure 12: Cadaver_1 thoracic strain distribution.

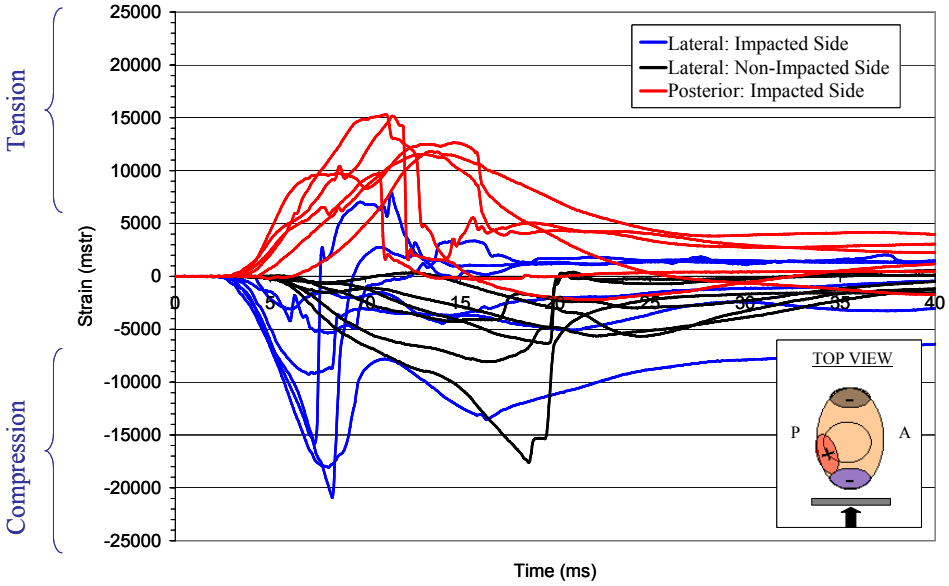

Figure 13**:** Cadaver_2 thoracic strain distribution.

CONCLUSIONS

The novel strain gaging technique presented in this study has allowed for the precise determination of the time of fracture for each rib. All rib fractures occurred within the first 33% compression of the thorax measured at rib 5. Lateral fractures on the impacted side occurred between 2% and 9% of compression measured at rib 5, posterior fractures on the impacted side occurred between 8% and 16% compression measured at rib 5, lateral fractures on the non-impacted side occurred between 28% and 32% compression measured at rib 5. In addition, for the first time, the exact point at which the different thoracic AIS scores occurred could be identified with the time of rib fracture data in side impact loading. Using rib fractures as the parameter for AIS scores, it was found that AIS=1 injuries occurred at a chest compressions of 2% to 3%, AIS=2 at 4% to 7%, and AIS=3 at 7% to 9% measured at rib five. Finally, the primary loading mode of the ribs varied with respect to thoracic region. The exterior portion of the ribs on the lateral region of both the impacted and non-impacted side was placed in compression, while the posterior region of the impacted side was placed in tension. The peak strain at failure ranged from -4192 mstr to -20194 mstr for lateral portions of the thorax and from 7491 mstr to 14142 mstr for posterior portions of the thorax. It is expected that the data from the current study will augment and clarify the foundation of thoracic injury risk functions for side impact.

ACKNOWLEDGEMENTS

The authors would like to thank Toyota Motor Corporation for providing the funding for this research.

REFERENCES

CAVANAUGH, J., HUANG, Y., and KING, A. (1993). Injury and Response of the thorax in Side Impact Cadaver Tests. SAE 933127. Society of Automotive Engineers, Warrendale, PA.

DUMA, S., STITZEL, J., KEMPER, A., MCNALLY, C., KENNEDY, E., and MATSUOKA, F. (2005). Non-censored rib fracture data from dynamic belt loading tests on the human cadaver thorax. Proc. 19th International Technical Conference on the Enhanced Safety of Vehicles. NHTSA, Washington, D.C.

MORGAN, R. , MARCUS, J. , and EPPINGER, R. (1986). Side Impact – the Biofidelity of NHTSA's Proposed ATD and Efficacy of TTI. Proc. 13th Stapp Car Crash Conference, pp. 27-40, Society of Automotive Engineers, Warrendale, PA.

PINTAR, F., YOGANANDAN, N., HINES, M., MALTESE, M., MCFADDEN, J., SAUL, R., EPPINGER, R., KHAEWPONG, N., and KLEINBERGER, M. (1997). Chestband Analysis of Human Tolerance to Side Impact. Proc. Forty-First Stapp Car Crash Conference, pp. 63-74, Society of Automotive Engineers, Warrendale, PA.

SAMAHA, R. and ELLIOTT, D. (2003). NHTSA Side Impact Research: Motivation for Upgraded Test Procedures, Eighteenth International Technical Conference on the Enhanced Safety of Vehicles, Paper No. 492, National Highway Traffic Safety Administration, Washington, D.C.

STITZEL, J., CORMIER, J., BARRETTA, J., KENNEDY, E., SMITH, E., RATH, A., and DUMA, S. (2003). Defining regional variation in the material properties of human rib cortical bone and its effect on fracture prediction. *Stapp Car Crash Journal*, 47: 243- 265.

VIANO, D. (1989). Biomechanical Responses and Injuries in Blunt Lateral Impact. Proc. 33rd Stapp Car Crash Conference, pp. 113-142, Society of Automotive Engineers, Warrendale, PA.

DISCUSSION

PAPER: **Determining Non-Censored Rib Fracture Data During Side Impact Loading**

PRESENTER: ***Andrew Kemper, Virginia Tech – Wake Forest Center for Injury Biomechanics***

QUESTION: *Erik Takhounts, NHTSA*
I have a question for you. You showed—I can't see it well from here, but you've shown that there are various levels of percent compression that you reach in a close lateral and whatever's next.

ANSWER: Posterior on the struck side.

Q: Posterior on the struck side, but the strain levels seem to be the same, approximately.

A: Right. Well, it depends on how close the fracture is to the strain gage. We can still pick up, within a reasonable distance, the rib fracture, but the rib fracture is—we would call it peak strain but not ultimate strain. It's just allowing us the timing of the measure. Unless it's really close to the gage or directly under the gage, I wouldn't go so far as to say that's—it's really not the actual, you know, ultimate strain.

Q: Alright. Well, how do you determine what the ultimate strain is at the fracture? Because right now, I have an impression that percent compression does not really relate to the strain levels because strain levels are approximately the same yet percent compression is changing. Do you see what I mean?

A: Yes, I see what you mean. Well, you could do—It'd be difficult, I guess, to determine the actual strain level. I guess you could do some correlations for, like, 3-point bending and trying to predict the strain at the actual peak bending?

Q: Or perhaps a model?

A: Or perhaps a model, yes.

Q: *Richard Kent, UVA*
First of all, Andrew, this is good stuff. I like the way you guys approach this. It looks like you're getting really good results. Could you answer the question for me, though, on how you deal with two fractures? If you get two fractures happening on a rib, are you still able to resolve those individually? Does it depend on where they are relative to the gages? Or, how do you deal with that somewhat randomness of multiple fractures on a rib?

A: It's kind of case-dependent as to where the rib fracture is relative to the gage. When there's multiple gages on the thorax, sometimes one will pick the first one up and another gage will pick up the second one. Also, adjacent ribs will also see jumps in strain and it has—Obviously, you have less confidence in that, but sometimes you would have—After that rib is actually fractured, more often than not, you probably can't see the second fracture.

Q: Okay. Yeah, we found that same sort of thing. Okay. And then one more question: It's interesting you're getting these injury levels to occur at quite a bit lower percent compressions than you would expect. For example, I think you're getting rib fracture onset at, I think, 2% (or something like that) compression. Can you explain that relative to, sort of, traditionally we wouldn't expect to see fractures happening at that low chest compression level? Does that have something to do with the interface or—? I mean, almost when I breathe, I get that much lateral chest compression. So I'm wondering how that's happening or if you have a reason for that.

A: I would think it has to do with the rate of loading, obviously, and then also the presence of the arm could focus the loading; you know, have a more direct impact on the chest as opposed to more distributed loading, which could be causing those very low levels of fracture.

Q: Interesting. Makes it harder for us to want to run sub-injury tests, to know what to do now. Alright. Thanks, Andrew.